

### Lifetime of the Tau Lepton

W. T. Ford, J. G. Smith, J. V. Allaby,<sup>(a)</sup> W. W. Ash, L. Baksay, H. R. Band, G. B. Chadwick, S. H. Clearwater, R. W. Coombes, M. C. Delfino, W. L. Faissler, M. W. Gettner, G. P. Goderre, Y. Goldschmidt-Clermont,<sup>(a)</sup> B. Gottschalk,<sup>(b)</sup> D. E. Groom, B. K. Heltsley, R. B. Hurst, J. R. Johnson, H. S. Kaye, K. H. Lau, H. Y. Lee, R. E. Leedy, S. P. Leung,<sup>(c)</sup> E. C. Loh, A. Marini, J. S. Marsh,<sup>(d)</sup> T. Maruyama, R. L. Messner, O. A. Meyer, S. J. Michalowski,<sup>(e)</sup> J. H. Moromisato, R. M. Morse, I. Peruzzi, M. Piccolo, R. Prepost, A. L. Read, Jr., K. Rich, D. M. Ritson, F. Ronga, L. J. Rosenberg, W. D. Shambroom, E. von Goeler, Roy Weinstein, D. E. Wiser, and R. W. Zdarko

*Department of Physics, University of Colorado, Boulder, Colorado 80309, and Laboratori Nazionali Frascati dell'Istituto Nazionale di Fisica Nucleare, Italy, and Department of Physics, Northeastern University, Boston, Massachusetts 02115, and Department of Physics and Stanford Linear Accelerator Center, Stanford University, Stanford, California 94305, and Department of Physics, University of Utah, Salt Lake City, Utah 84112, and Department of Physics, University of Wisconsin, Madison, Wisconsin 53706*  
(Received 17 May 1982)

From three-prong decays of  $\tau$  leptons produced in the MAC detector at PEP, the lifetime of the  $\tau$  is determined to be  $(4.9 \pm 2.0) \times 10^{-13}$  sec.

PACS numbers: 14.60.Jj, 13.35.+s

Determination of the  $\tau$  lepton lifetime permits a straightforward test of the weak charged-current coupling of the  $\tau$  system. In the present experiment three-prong decays in flight of monoenergetic taus, produced by electron-positron annihilations at PEP, were used to measure the  $\tau$  lifetime.

The MAC detector has been described elsewhere.<sup>1</sup> The analysis presented here depends most directly upon the central tracking chamber, which consists of ten layers of drift wires in a solenoidal magnetic field of 5.7 kG. The radii of the innermost and outermost layers are 12 and 45 cm, respectively. The range of angles subtended by all ten layers is  $23^\circ \leq \theta \leq 157^\circ$ . Each cell contains a double sense-wire pair connected to differential electronics so that drift distance is determined without right-left ambiguity. The wires in four of the layers are axial; these are interspersed with six stereo layers at plus and minus three degrees to determine axial positions. The point measurement accuracy is about 200  $\mu$ m. Between the interaction point (IP) and the first drift layer are the vacuum pipe and the drift-chamber wall which total 0.036 radiation lengths at an average radius of 9.4 cm.

The central drift chamber is surrounded by electromagnetic and hadronic calorimeters, scintillation counters, and muon tracking chambers, which were used in the present experiment

for triggering and event selection. The acceptance of these detector elements is greater than 95% of the solid angle.

Data for this measurement came from an exposure of 16 900 inverse nanobarns, of which 15 000 were taken at a center-of-mass energy of 29 GeV, the rest at 28 GeV. Events having at least four reconstructed prongs and sphericity<sup>2</sup> less than 0.1 were divided into two jets by the plane perpendicular to the sphericity axis. Selected events had at least one three-prong jet, accompanied by a jet of one, two, or three prongs, in both cases excluding any tracks which had been fitted as photon conversions in the vacuum pipe or chamber wall. The sum of charges of the tracks was required to be zero, except for those events having two reconstructed tracks opposite a three-prong decay candidate with evidence, upon visual inspection, of a third track which failed the reconstruction.

Each three-prong decay candidate was subject to the following track quality conditions: an average of at least seven hits per track,  $\chi^2$  for the vertex fit less than 15 for three degrees of freedom, and net charge equal  $\pm 1$ . Events passing these criteria were examined visually; about half were rejected as obvious background, mostly single-photon or two-photon multihadrons, often containing extra unreconstructed tracks.

Remaining backgrounds were (1) Bhabha elec-

tron pairs with an additional pair from conversion of a radiated photon that failed to be reconstructed as such, (2)  $ee\tau\tau$  and  $ee$  (hadron) events with undetected electrons, (3) beam-gas interactions, and (4) four- and six-prong multihadron events.

To remove these backgrounds the following additional requirements were imposed: (1) the total energy computed from the calorimeter pulse heights less than the pure-electromagnetic equivalent of 24 GeV, to eliminate converting radiative electron pairs; (2) charged-track sphericity less than 0.03, which Monte Carlo calculations showed would retain almost all  $\tau$  pairs while removing a large fraction of beam-gas,  $ee\tau\tau$ , and  $ee$  (hadron) events; (3) the net momentum of each triplet greater than 4 GeV/c to discriminate further against  $ee\tau\tau$  events; and (4) the larger of the two jet invariant masses, determined from energy flow in the calorimeters, less than 4.5 GeV/c<sup>2</sup> (the invariant-mass distribution of the visible  $\tau$  decay products is bounded by  $m_{\tau} \approx 1.8$  GeV, broadened by the hadron cascade in the calorimeter; from the corresponding distribution for detected multihadron events we found that about 90% were excluded by this cut, independent of their charged multiplicity).

There are 135 events, containing 139 reconstructed three-prong decays, which pass the selection criteria. To gain confidence that nearly all of these are  $\tau$  pairs we have compared with calculation the distributions in the relevant kinematic variables, such as total energy and its charged-particle component, momenta of the single- and three-prong decay products, three-prong mass, production angle, and branching ratios for the decay opposite each three-prong decay. In each case we find good agreement. From Monte Carlo calculations we estimate that seven multihadron and one  $ee\tau\tau$  events remain as background in the sample.

By  $\chi^2$  minimization, the fitting procedure for the decay vertices produced values for the coordinates of the decay point and their correlated errors. The production point was taken to be the center of the beam intersection volume. The coordinates of this point were determined by reconstructing the Bhabha scattering events recorded simultaneously with the  $\tau$  pairs, and averaging the fitted vertex coordinates over the events in each data run. The beam position stability over extended data-taking periods was found to be such that the effective measured beam size was about 0.5 mm (rms) in the vertical dimension and 0.7

mm in the horizontal. Since the longitudinal beam bunch length was much larger (about 1.5 cm), the decay path was determined from its projection on the plane perpendicular to the beam. In this plane the distance between the vertex and the IP and its error were projected onto the momentum vector of the triplet, which is approximately that of the parent  $\tau$ . Figure 1 shows the distribution in flight path error. Decays having an error larger than 8 mm were excluded from the subsequent analysis.

The decay path distribution is shown in Figs. 2(a) and 2(b). Each event has been entered into the histogram of Fig. 2(a) with unit weight, and into that of Fig. 2(b) weighted by the reciprocal squared error. The weighting procedure optimizes the information extracted from the data on the sample mean, but tends to create bias, since the error is a function of distance from the measurements. We have retained both distributions as a check on this effect.

In both distributions of Fig. 2 there is a clear indication of a nonzero decay length. Although the measurement error is larger than the decay length,  $\lambda$ , the value of  $\lambda$  can be deduced from the sample mean. If we assume that the observed distribution is the convolution of an exponential decay curve with the experimental resolution function, which itself may have a nonzero mean value or bias  $x_b$ , then the value of  $\lambda$  and its error,  $\sigma_\lambda$ , are unfolded

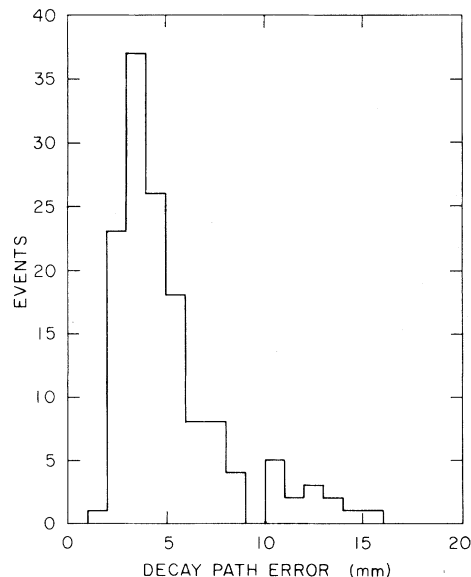


FIG. 1. Distribution of the decay path length error from vertex fits to three-prong  $\tau$  decays.

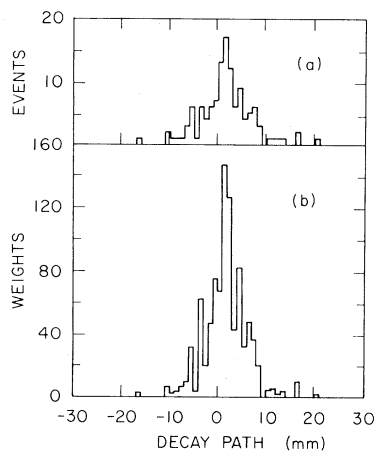


FIG. 2. Decay length distribution for  $\tau$  decays: (a) unweighted, (b) weighted by the reciprocal squared error.

according to

$$\begin{aligned}\lambda &= \langle x \rangle - x_b, \\ \sigma_{\lambda}^2 &= (\sigma_x^2 - \lambda^2)/N,\end{aligned}\quad (1)$$

where  $\langle x \rangle$  and  $\sigma_x$  are the mean and standard deviation of the observed distribution, and  $N$  is the number of events.

From a Monte Carlo calculation of the distribution in vertex position expected for taus of zero lifetime we determined the resolution function for the flight path measurement. A nonzero bias was found, as given in Table I for both unweighted and weighted distributions. We attribute this result to the  $\chi^2$  fitting procedure which, in effect, computes a weighted average of the intersection points formed by three pairs of tracks in each triplet. The weight given to each intersection tends to decrease with its distance from the

TABLE I. Summary of decay path and bias values, in millimeters. See text for definition of the weights referred to in the column headings.

	Unweighted	Weighted
$\tau$ sample		
$\tau$ raw $\langle x \rangle$ ( $\sigma_x$ )	1.57 (5.48)	1.75 (4.43)
Monte Carlo $\langle x \rangle = x_b$	$0.50 \pm 0.01$	$0.55 \pm 0.01$
$\tau$ corrected $\lambda$	$1.07 \pm 0.49$	$1.20 \pm 0.39$
Control sample		
raw $\langle x \rangle$ ( $\sigma_x$ )	0.31 (4.86)	0.68 (4.03)
$x_b$	$0.30 \pm 0.10$	$0.30 \pm 0.08$
$\lambda_{\text{eff}}$	$0.01 \pm 0.21$	$0.38 \pm 0.17$
$\lambda_{\text{eff}}$ (calc)	$0.18 \pm 0.08$	

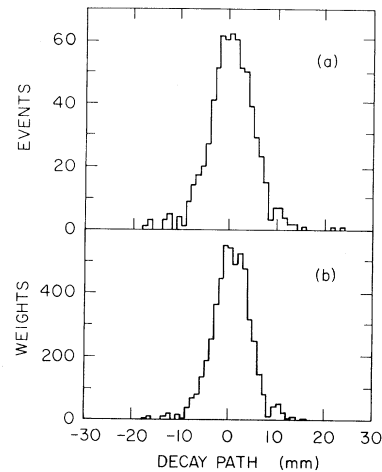


FIG. 3. Decay length distribution for control events: (a) unweighted, (b) weighted by the reciprocal squared error.

measured track points, resulting in a bias of the triplet vertex toward these points. Variation in the Monte Carlo process of the efficiency and noise rate of the tracking chamber has been shown to produce no significant change in the magnitude of the bias.

From the data of the first two lines of Table I together with Eq. (1) we find the corrected flight path values entered in the third line. The results for unweighted and weighted averages are in good agreement. Analysis of Monte Carlo events generated with the observed decay length gave the same decay path distribution as the data.

As a check on the calculated resolution function, we have constructed a sample of tau-like events from multihadron events observed in the detector. Random triplets were chosen from within the hadron jets which met requirements adjusted to simulate  $\tau$  decays as nearly as possible. In particular, the decay-path error distribution for the events was made to agree with the one for taus (Fig. 1). The decay-path distributions for these events are given in Figs. 3(a) and 3(b) and the mean values are entered in Table I under the heading "control sample," along with Monte Carlo results for the bias (determined by suppressing decays in the multihadron Monte Carlo simulation), and the effective decay length after subtraction of the bias,  $\lambda_{\text{eff}}$ . The results are to be compared with the contribution expected from hadronic decays, calculated by setting the drift-chamber resolution equal to zero in the Monte Carlo calculation, which appears in the last line of Table I. It can be seen that the measured and

calculated effective decay lengths agree within about 0.2 mm. Variations of the above control sample were also studied. Considering the consistency of all the data for both  $\tau$  and control events we have assigned a systematic uncertainty of 0.3 mm to the decay path measurement.

Taking the  $\tau$  mass to be<sup>3</sup> 1.782 GeV, and the average beam energy for this experiment of 14.5 GeV, we find for the lifetime

$$\tau_{\tau} = (4.9 \pm 2.0) \times 10^{-13} \text{ sec.}$$

Here we have used the weighted mean decay path from Table I, and have added the 0.3-mm systematic uncertainty in quadrature with the statistical error given there. The prediction from  $\tau$ - $\mu$  universality is given by

$$\tau_{\tau} = (m_{\mu}/m_{\tau})^5 \tau_{\mu} b_e = (2.8 \pm 0.2) \times 10^{-13} \text{ sec,}$$

where  $b_e$  is the branching fraction for  $\tau \rightarrow e\nu\bar{\nu}$ ,  $0.176 \pm 0.016$ .<sup>4</sup> Previous published measurements include values of<sup>5</sup>  $(4.6 \pm 1.9) \times 10^{-13}$  and<sup>6</sup>  $(-0.25 \pm 3.5) \times 10^{-13}$  sec, consistent with the result reported here.

This work was supported in part by the Department of Energy under contracts No. DE-AC02-76ER02114, No. DE-AC03-76SF00515, and No. DE/AC02-76ER00881, by the National Science Foundation under Contracts No. NSF-PHY80-

06504, No. NSF-PHY79-20020, and No. NSF-PHY79-20821, and by the Istituto Nazionale di Fisica Nucleare.

(a)Permanent address: CERN, Geneva, Switzerland.

(b)Present address: Cyclotron Laboratory, Harvard University, Cambridge, Mass. 02438.

(c)Present address: 20 Caine Road, Hong Kong, B. C. C.

(d)Present address: SRI International, Menlo Park, Cal. 94025.

(e)Present address: Mechanical Engineering Department, Stanford University, Stanford, Cal. 94305.

<sup>1</sup>MAC Collaboration, in Proceedings of the International Conference on Instrumentation for Colliding Beams, edited by W. Ash, Stanford Linear Accelerator Center Report No. SLAC-PUB-2894, 1982 (to be published).

<sup>2</sup>Sphericity is defined in, for example, G. Hanson *et al.*, Phys. Rev. Lett. **35**, 1609 (1975).

<sup>3</sup>W. Bacino *et al.*, Phys. Rev. Lett. **41**, 13 (1978).

<sup>4</sup>C. A. Blocker *et al.*, Stanford Linear Accelerator Center Report No. SLAC-PUB-2820, 1981 (unpublished).

<sup>5</sup>G. J. Feldman *et al.*, Phys. Rev. Lett. **48**, 66 (1982).

<sup>6</sup>J. G. Branson (TASSO Collaboration), in *Proceedings of the 1981 International Symposium on Lepton and Photon Interactions at High Energies, Bonn, 24-29 August 1981*, edited by W. Pfeil (Physikalisches Institut, Universität Bonn, Bonn, Germany, 1981).

## Fermi-Gamow-Teller Mixing in the Allowed Isospin-Hindered Positron Decay of $^{56}\text{Co}$

J. L. Groves, W. P. Lee,<sup>(a)</sup> A. M. Sabbas, M. E. Chen, P. S. Kravitz,  
L. M. Chirovsky,<sup>(b)</sup> and C. S. Wu

*Physics Department, Columbia University, New York, New York 10027*

(Received 23 March 1982)

A new high-precision measurement of the asymmetry coefficient,  $A_{\beta}$ , for the positron decay of polarized  $^{56}\text{Co}$  is reported:  $A_{\beta} = +0.359 \pm 0.009$ . If one assumes the  $V-A$  form of the weak interaction and time-reversal invariance, the Fermi-Gamow-Teller mixing ratio,  $y = C_V M_F / C_A M_{GT}$ , is then  $-0.091 \pm 0.005$ . Since  $y$  is nonzero and isospin is not conserved,  $^{56}\text{Co}$   $\beta^+$  decay is a good candidate for sensitive time-reversal invariance tests of the weak interaction.

PACS numbers: 23.40.Hc, 27.40.+k

The allowed isospin-hindered ( $J^{\pi} \beta^{\pm} J^{\pi}$ ,  $T \rightarrow T \pm 1$ )  $\beta$  transitions in nuclei<sup>1</sup> are of particular interest for studies of isospin conservation of nuclear forces<sup>2</sup> and for time-reversal invariance (TRI) tests of the weak interaction.<sup>3</sup> Fermi transitions require  $\Delta T = 0$ , and consequently, a nonzero value of the Fermi to Gamow-Teller mixing ratio,<sup>1</sup>  $y = C_V M_F / C_A M_{GT}$ , violates isospin conservation.

In TRI tests in nuclear  $\beta$  decay, the magnitudes of  $T$ -odd correlations are proportional to  $y$ . Furthermore, Barroso and Blin-Stoyle<sup>3</sup> have suggested that possible  $T$ -nonconserving effects in allowed isospin-hindered  $\beta$  transitions may be amplified by a factor of  $10^2$ . Consequently, precise measurements of  $y$  for these  $\beta$  transitions are of fundamental importance.